JCEC
THE JOURNAL OF ENGINEERING AND EXACT SCIENCES

OPEN ACCESS

The Journal of Engineering and Exact Sciences – jCEC, Vol. 08 N. 04 (2022)
journal homepage: https://periodicos.ufv.br/jcec
eISSN: 2527-1075
ISSN: 2446-9416

Numerical simulation of optimal inlet air temperature of a forced convective fish cabinet rotary dryer

Simulação numérica da temperatura do ar de entrada ideal de um secador rotativo de armário de peixes convectivo forçado

Article Info:
Article history: Received 2022-02-04 / Accepted 2022-04-19 / Available online 2022-04-21
doi: 10.18540/jcecvl8iss4pp14157-01e

Emmanuel Obiani Akari
ORCID: https://orcid.org/0000-0001-5910-4144
University of Lagos, Nigeria
E-mail: akariobiani42@gmail.com
Ibrahim Ademola Fetuga
ORCID: https://orcid.org/0000-0002-1943-4234
University of Lagos, Nigeria
E-mail: fetugaebraheem@gmail.com
Olabode Thomas Olakoyejo
ORCID: https://orcid.org/0000-0001-9942-1339
University of Lagos, Nigeria
E-mail: oolakoyejo@unilag.edu.ng
Manasseh Babale Shitta
ORCID: https://orcid.org/0000-0001-6070-5748
University of Lagos, Nigeria
E-mail: shitta@nceec.gov.ng
Omotayo Oluwatusin
ORCID: https://orcid.org/0000-0003-3683-2848
University of Lagos, Nigeria
E-mail: ooluwatusin@unilag.edu.ng
Joshua Kolawole Gbegudu
ORCID: https://orcid.org/0000-0003-2417-2520
University of Lagos, Nigeria
E-mail: jk.gbegudu@gmail.com
Antônio Marcos de Oliveira Siqueira
ORCID: https://orcid.org/0000-0002-7088-3211
Federal University of Viçosa, Brazil
E-mail: antonio.siqueira@ufv.br

Resumo
A dinâmica do fluido computacional foi aplicada na previsão do efeito da temperatura da entrada no tempo de secagem dos peixes em um secador de armário. Após a conclusão da simulação, obteve-se a distribuição de temperatura do ar (domínio fluido) dentro do seco em diferentes temperaturas do ar de entrada e intervalos de tempo. As temperaturas do ar de entrada variando de 35ºC a 55ºC foram simuladas para um intervalo de tempo de 10 minutos a 120 minutos, de modo a examinar a influência da temperatura da entrada no processo de secagem dos peixes. Com base nessa faixa de temperatura, observou-se que o tempo ideal de secagem para o peixe que satisfaz a condição de secagem eficiente de peixes para todas as cinco temperaturas de ar de entrada do peixe é de 70 minutos. Além disso, pode-se observar que leva cerca de 120 minutos para a temperatura do ar de entrada de 50 graus Celsius atingir uma temperatura de secagem do gabinete de 316K (43°C)

enquanto leva apenas 70 minutos para a temperatura do ar de entrada de 55 graus Celsius atingir a mesma temperatura sob a mesma condição.
Palavras-chave: Dinâmica de Fluidos Computacionais. Armário Do Secador Rotativo. Taxa de secagem, ANSYS CFX. temperatura do ar de entrada.

Abstract
Computational fluid dynamics was applied in the prediction of the effect of inlet temperature on the drying time of fish in a cabinet rotary dryer. On completion of the simulation, the temperature distribution of the air (fluid domain) within the drier at different inlet air temperatures and time intervals was obtained. Inlet air temperatures ranging from 35ºC to 55ºC was simulated for a time interval of 10 minutes to 120 minutes so as to examine the influence of inlet temperature on the drying process of fish. Based on this temperature range, it was observed that the ideal drying time for the fish which satisfies the condition for efficient fish drying for all five inlet air temperatures of the fish is 70 minutes. Furthermore, it can be observed that it takes about 120 minutes for the inlet air temperature of 50 degrees Celsius to attain a cabinet drying temperature of 316K (43°C) while it takes only 70 minutes for the inlet air temperature of 55 degrees Celsius to attain the same temperature under the same condition.
Keywords: Computational Fluid Dynamics. Cabinet Rotary Dryer. Drying rate. ANSYS CFX. Inlet air temperature.

1. Introduction

Drying food is a preservation method that reduces or stop the growth of bacteria, yeast and mold by removing water. The process of removing water is referred to as dehydration, this process has been widely used for this purpose since ancient times. Water is traditionally removed by evaporation (air drying, sun drying, fumigation, or wind drying) (Abd El-Hay, 2022; Zhu et al., 2022).

If fresh fish is not preserved early and properly, it deteriorates rapidly because of the high content of its moisture. Fish drying is a complicated heat and mass transfer process that involves the transfer of moisture to the fish's surface and subsequent evaporation of the moisture through heating. Drying prevents the growth of food spoilage microorganisms, which survive in the presence of an adequate amount of water. Drying is an essential process in many food sectors, and vast amounts of food are dried in many agriculturally active countries to extend shelf life, cut packing costs, and reduce transportation weight. Fish and meat are perishable food products that can contain up to 80% moisture (Çetinkaya, Ceylan, Meral, Kılıçer, & Altay, 2021; Darvishi, Azadbakht, Rezaeiasl, & Farhang, 2013; Rathod et al., 2021; Singh, Mittal, & Benjakul, 2022; Tavares et al., 2021). These food products are prone to spoilage and contamination by micro-organisms unless preserved or processed. The high temperature characteristics of the tropics lead to the growth of the bacteria and enhance the spoilage of these food products (Dabadé Et Al., 2015; Shamshad, Kher-Un-Nisa, Riaz, Zuberi, & Qadri, 1990). When the moisture content of fresh fish falls below 25%, there is a reduction in the survival rate of the micro-organisms and the enzyme activities (Horner, 1997). The moisture content of the fish must be reduced to 15% or less during storage to prevent the growth of mold (Daramola, Fasakin, Adeparusi, & Daramola, 2016; Horner, 1997; Shenderyuk & Bykowski, 2020).

To avoid the problem of post-harvest losses in fish production, a lot of research work on fish drying has been carried out. (Legendre, 2011a, 2011b) designed and tested an artificial dryer of 2-ton capacity and the Cambodian fish experimental data from it showed a good drying rate and suggested a temperature of 26.7oc good enough for fish drying by maintaining the air velocity of 1.5 m/s to 22 m/s, The initial drying phase should be long enough to reduce the moisture content of the fish to about 65-69 percent, and the process should be finished by subsequent 12-hour drying periods with the relative humidity of the drying atmosphere at around 50-55 percent. (Miketinac, Sokhansanj, & Tutek, 1992) developed five models for heat and mass transfer in drying a thin layer

of barley and discovered that the heat transfer coefficient varied from 43 to 59 W/m^2 K in relying on the drying model. (Tesfamariam, Bayray, Tesfay, & Hagos, 2015) designed, manufactured, and tested an indirect passive convectional solar dryer and dryer chamber, and discovered an improvement in the performance of the collector by using a corrugated absorber to crate turbulence airflow and a good insulator to minimize heat losses. (Brasil Maia et al., 2012) numerically simulated the airflow inside a hybrid solar-electrical dryer with the ANSYA-CFX 11 code, which was validated and predicted the behavior of airflow inside the device with prescribe temperature and velocities. (Tzempelikos et al., 2013) developed and tested a fluid flow model for a new laboratory convective (LC) dryer. They concluded that better air distribution in the dryer improved performance and inferred the turbulence parameters inside the dryer by standard k-ϵ turbulence model. (Dasin, Godi, & Kingsley, 2015) designed, developed, and evaluated the performance of a multipurpose passive solar food dryer. They investigated the drying rate of the dryer for fish, pepper, yam, and tomatoes. They further revealed that the dryer efficiency for fish is 6.6% and that the system is more efficient for drying yam than tomatoes, pepper, and fish. (Pelegrina, Elustondo, & Urbicain, 1998, 1999) examined the effect of recycled exhaust air on a rotary dryer for drying vegetables. It was reported that the energy usage was minimized by mixing recycled exhaust air with fresh air. They further stated that to retain the quality of the vegetables, a smaller proportion of the recycled exhaust air must be used in the mixture. The rotating cylindrical drier for drying apricot was fabricated and examined by (Sarsilmaz, Yildiz, & Pehlivan, 2000). They revealed that the fabricated dryer doubles the rate of drying the Sugar piece-type apricots to attain a moisture level of 25% as compared to drying on an open sheet. The V-groove air collection absorber was used by (Li et al., 2006) to fabricate a forced convection dryer for drying salted greengages. Spread wet-salted greengages on the top two trays and semi-dry greengages on the remaining trays to improve thermal efficiency. (Smolka, Nowak, & Rybarz, 2010) simulated different configurations to improve temperature uniformity in the drying chamber and it was reported in their work that the numerical results obtained were extremely close to the experimental data.

The use of the cabinet rotary dryer, which is a type of mechanical fish dryer, is an efficient and fast way of carrying out fish drying on a small scale. Computational Fluid Dynamics (CFD) applied to the simulation and optimization of drying processes has assumed a leading role in the thermal design of forced convection cabinet dryers. In all the previous work carried out by researchers in this field, configurations of different shapes were considered, varying constraints put in place aimed at increasing the performance of the drying compartment. However, the air that blows the moisture content away from the element to be dried has received little or no attention, hence this called for the need for this work. This research therefore aims to look at the effect of varying the air inlet temperature on the drying process of the fish using a forced convection in a cabinet rotary dryer.

2. Methodology

This research used the application of various thermodynamic and CFD processes which are very pertinent in the transient analysis of fish drying to simulate the inlet air temperature. The procedures taken in carrying out the CFD simulation are given below:

Pre-Processing: This preliminary setup process requires the modeling of the control volumes that make up the entire computational geometry using CATIA V5 software. These include the cabinet body, the fish geometry, and the fluid domain. Individual models are imported into ANSYS Workbench for further processing when the modeling operation has been completed. The individual model geometries are now meshed to generate the computational grid (mesh elements) with the ANSYS ICEM CFD Mesher. The individual meshes were exported and saved for further processing in ANSYS CFX. The boundary conditions, domains, domain interfaces, solver settings and material properties of the fish and the air are setup in ANSYS CFX.

Processing: ANSYS CFX-Solver processes the setup data that has been inputted into CFX-Pre. A steady state solution of the problem is generated prior to the commencement of the transient simulation of the problem. This was carried out so as to derive initial values for the flow field with which the CFX-Solver would utilize as an initial guess value for all flow quantities (temperature, pressure, velocity). The time variations for the simulations were in an increment of 10 minutes. The first simulation was carried out at 10 minutes and then increased gradually till it gets to 120 minutes for different inlet drying temperatures which ranges from 35oC to 55oC at the interval of 5oC.

Post-Processing: The results of the simulation are post-processed using ANSYS CFD-Post and Microsoft Excel applications. The temperature, velocity and turbulence distribution inside the cabinet dryer are visualized using contour plots and planes at different positions in the dryer. The drying temperature and velocity results at specific zones inside the dryer was also obtained and tabulated so as to assess the drying temperature distribution in the dryer with a view to ascertaining the optimum drying temperature/time range suitable for the drying process.

2.1 Geometry Description

As shown in Figure 1, the cabinet dryer body is a solid domain. It measures 1m width by 1 m breadth and by 1m height. It is made of carbon (mild) steel, and the entire body of the dryer is assumed to be adiabatic so as to prevent heat interaction with the environment. There are two circular openings each on all four edge ends of the dryer to allow for the inflow of hot air into the chamber, and also a circular opening at the dryer top to allow for the escape of heat from the dryer. The fish model is assumed to be of an elliptical shape and is placed on a rotating table, which enables the proper circulation of hot air from the bottom of the rotating table, which is porous. Table 1. shows the dimensions of the cabinet rotary dryer.

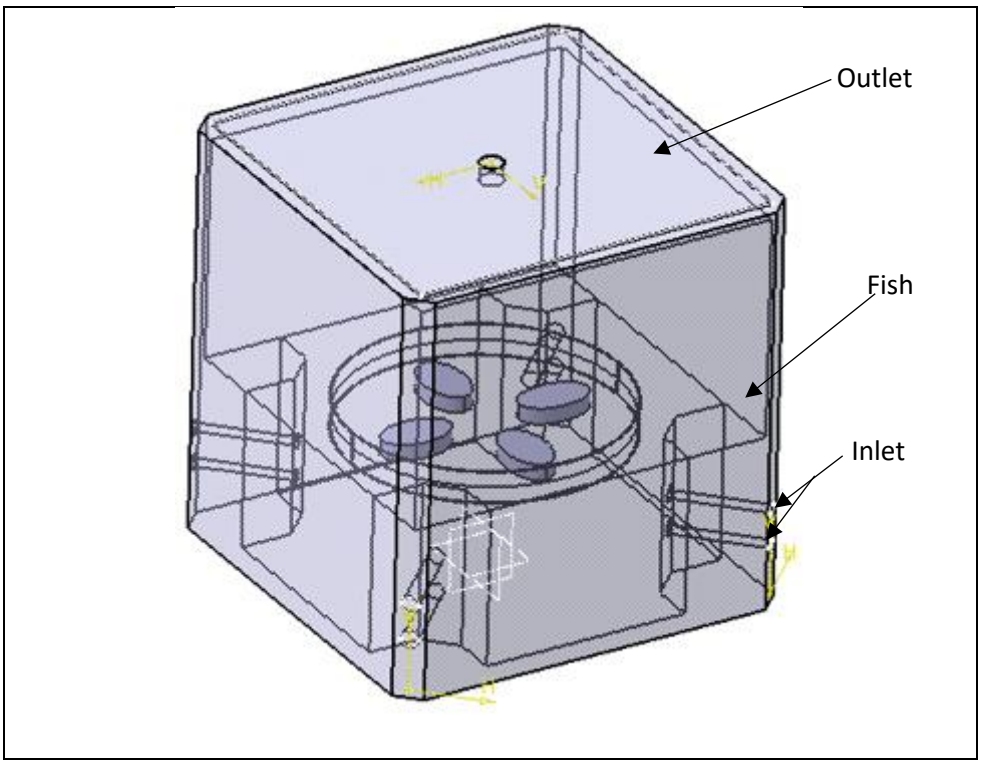

Figure 1- Complete Computational domain assembly of the cabinet rotary dryer

Table 1- Dimensions of the cabinet rotary dryer

Parameters	Cabinet Rotary Dryer
Dimension	1m length x 1m width x 1m height
Gross rotary dryer volume	$1m^3$
Net Volume of rotary dryer (Volume of internal fluid region)	0.76 m^3
Number of inlets	8
Diameter of each inlet	0.04m
Number of outlets	1
Internal fluid in dryer before drying process	Air at 25C

2.2 Mesh Generation

As displayed in Figure 2(a) -2(d), ANSYS ICEM CFX Mesher was used to generate the computational grid or mesh for the different parts of the cabinet dryer domains, and the individual mesh files were saved. Using the Automatic Inflation feature settings, the meshing was done to capture the flow mechanics in several distinct geometry faces such as edges, concentric faces, and smaller apertures. Tetrahedral, pyramidal, wedge, and hexahedral element types are among the mesh elements formed. The mesh quality of all dryer domains was high, which was ensured in order to provide a good flow forecast.

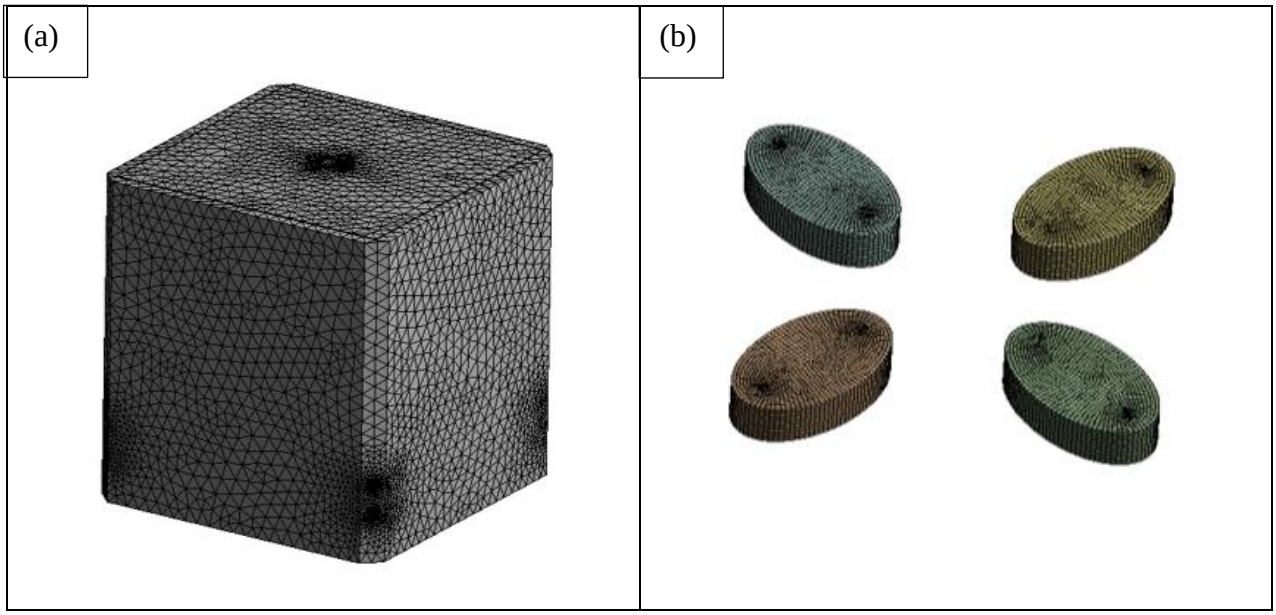

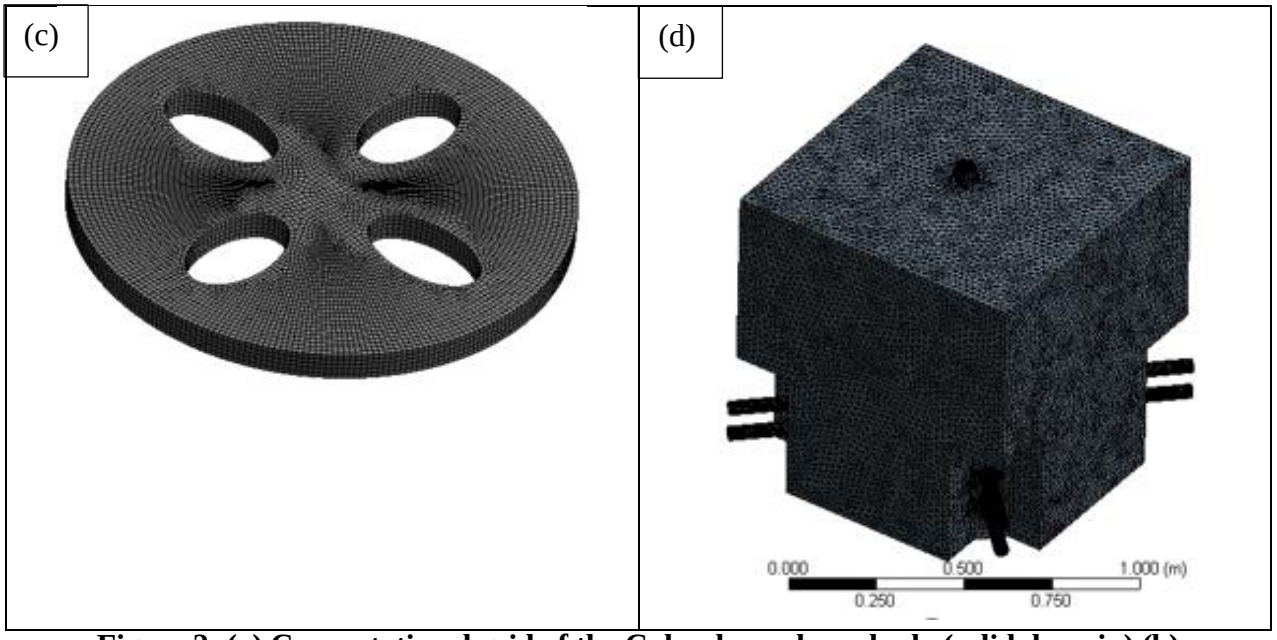

Figure 2- (a) Computational grid of the Cube shape dryer body (solid domain) (b) Computational grid of the Fish (solid domain) (c) Computational grid of the Fish boundary (fluid domain) (d) Computational grid of the Internal Dryer Air Volume (fluid domain)

2.3 Problem Formulation

This section will look into the governing equations, boundary conditions, and assumptions used. The set of equations solved by ANSYS CFX is the unsteady Navier-Stokes equations in their conservation form. The following assumptions were taken into account when simulating the drying process:

1. The heat transfer between the fish and the hot air convective
2. Turbulent flow of hot air into the drying chamber
3. The drying air is incompressible and of low Mach number.
4. The initial temperature inside the dryer is assumed to be ambient prior to the commencement of the drying process.
5. The effect of radiation is negligible.
6. The shape of the fish is unaltered during the drying process.
7. Rotary table is assumed to be fully porous for maximum flow of hot air to the fish.
8. No slip velocity boundary condition at the wall of the air within the chamber.
9. Transient and 3- dimensional flow.

Using the mass, momentum, and energy conservation laws, we can derive the continuity equation, momentum equation, and energy equation as shown below.

Continuity equation

$$\frac{D\rho}{Dt} + \rho \frac{\partial U_i}{\partial x_i} = 0 \quad (1)$$

Momentum equation

$$\rho \frac{\partial U_j}{\partial t} + \rho U_i \frac{\partial U_j}{\partial x_i} = -\frac{\partial P}{\partial x_j} - \frac{\partial \tau_{ij}}{\partial x_i} + \rho g_j \quad (2)$$

Where, $\tau_{ij} = -\mu\left(\frac{\partial U_j}{\partial x_i} + \frac{\partial U_i}{\partial x_j}\right) + \frac{2}{3}\delta_{ij}\mu\frac{\partial U_k}{\partial x_k}$ (3)

Energy equation

$$\rho c_\mu \frac{\partial T}{\partial t} + \rho c_\mu U_i \frac{\partial T}{\partial x_i} = -P\frac{\partial U_i}{\partial x_i} + \lambda\frac{\partial^2 T}{\partial x_i^2} - \tau_{ij}\frac{\partial U_j}{\partial x_i} \quad (4)$$

Turbulence equation
k-epsilon turbulence model
In the $k-\varepsilon$ model, two new variables are included into the system of equations. The turbulence kinetic energy is denoted by k, and the rate at which velocity fluctuations dissipate is denoted by ε. The continuity equation is further written as follows:

$$\frac{\partial \rho}{\partial t} + \frac{\partial}{\partial x_j}\left(\rho U_j\right) = 0 \quad (5)$$

and the momentum equation is then:

$$\frac{\partial p U_i}{\partial t} + \frac{\partial}{\partial x_j}\left(\rho U_i U_j\right) = -\frac{\partial P'}{\partial x_i} + \frac{\partial}{\partial x_j}\left[\mu_{eff}\left(\frac{\partial U_i}{\partial x_j} + \frac{\partial U_j}{\partial x_i}\right)\right] + S_M \quad (6)$$

Where the sum of body forces is represented by S_M, effective viscosity accounting for turbulence is denoted by μ_{eff} and the modified pressure is denoted by P'. Thus, $\mu_{eff} = \mu + \mu_t$
where turbulence viscosity is represented by μ_t. The $k-\varepsilon$ model implies that turbulence viscosity is proportional to turbulence kinetic energy and dissipation, as follows:

$$\mu_t = C_\mu \rho \frac{k^2}{\varepsilon} \quad (7)$$

Thus,

$$\frac{\partial(\rho k)}{\partial t} + \frac{\partial}{\partial x_j}\left(\rho U_j k\right) = \frac{\partial}{\partial x_j}\left[\left(\mu + \frac{\mu_t}{\sigma_k}\right)\frac{\partial k}{\partial x_j}\right] + P_k - \rho\varepsilon + P_{kb} \quad (8)$$

$$\frac{\partial(\rho\varepsilon)}{\partial t} + \frac{\partial}{\partial x_j}\left(\rho U_j \varepsilon\right) = \frac{\partial}{\partial x_j}\left[\left(\mu + \frac{\mu_t}{\sigma_\varepsilon}\right)\frac{\partial \varepsilon}{\partial x_j}\right] + \frac{\varepsilon}{k}\left(C_{\varepsilon 1}P_k - C_{\varepsilon 2}\rho\varepsilon + C_{\varepsilon 1}P_{\varepsilon b}\right) \quad (9)$$

where $C_{\varepsilon 1}$, $C_{\varepsilon 2}$, σ_k and σ_ε are constants.
The influence of the buoyancy forces, which are expressed below, is represented by P_{kb} and $P_{\varepsilon b}$. P_k is the turbulence produced by viscous forces, which is expressed as follows;

$$P_k = \mu_t\left(\frac{\partial U_i}{\partial x_j} + \frac{\partial U_j}{\partial x_i}\right)\frac{\partial U_i}{\partial x_j} - \frac{2}{3}\frac{\partial U_k}{\partial x_k}\left(3\mu_t\frac{\partial U_k}{\partial x_k} + \rho k\right) \quad (10)$$

Table 2- Material properties for the air, fish and dryer body

Material Name	(Air at 25°C) Ambient Air	Fish	Dryer body
Material Description	Air at 25°C and 1 atm (dry)	Tropical Fish	Steel
Thermodynamic state	Gas	Solid	Solid
Molar Mass	28.96 kg/kmol	178.976 kg/kmol	55.85 kg/kmol
Density	1.185 kgm^{-3}	1055 kgm^{-3}	7854 kgm^{-3}
Specific Heat Capacity	1004.4 J/(kg/K)	3540 J/(kg/K)	4340 J/(kg/K)
Dynamic viscosity	1.832×10^{-5} kg/ms	-	-
Thermal conductivity	2.61×10^{-5} W/mK	0.282744 W/mK	60.5 W/mK
Buoyancy properties	$0.003356k^{-1}$	-	-

Boundary Conditions

Boundary conditions used are given in Table 3a and Table 3b

Table 3a- Domain settings and Boundary conditions for the internal air volume, fish boundary and fish domain

	Internal Air Volume	Fish Boundary Fluid Domain	Fish Solid Domain
Domain type	Fluid domain	Fluid domain	Solid domain
Material	Air at 25oC	Air at 25oC	Fish
Morphology	Continuous fluid	Continuous fluid	Continuous Solid
Reference pressure	1 atm	1 atm	1 atm
Buoyancy model	Non buoyant	Non buoyant	Non buoyant
Domain motion	Stationary	Rotating, ω =5 rev/min at coordinate axis of Global Y	Rotating, ω =5 rev/min at coordinate axis of Global Y
Mesh deformation	None	None	None
Heat transfer	Total Energy	Total Energy	Thermal Energy
Turbulence	K-Epsilon	K-Epsilon	-
Wall function	scalable	Scalable	-

Table 3b- Domain settings and Boundary conditions for the inner air fluid- fish boundary interface

INNER AIR FLUID DOMAIN – FISH BOUNDARY DOMAIN INTERFACE	
Interface Type	Fluid – Fluid
Interface name	Inner Air region – Fish boundary domain interface
Interface side 1	Inner Air Fluid Domain
Interface side 2	Fish Boundary
Interface models	General connection
Frame Change/Mixing Model	Frozen Rotor
Pitch Change (option)	Specified pitch angles
Pitch angle side 1	360 degrees
Pitch angle side 2	360 degrees
Additional Interface models	Mass and Momentum (Conservative interface flux) Interface model (none)
Mesh Connection	GGI

3. Numerical Procedure

The advection scheme, transient scheme, turbulence numeric, and output transient results settings were all entered into the CFX-Solver for the simulation. The minimum and maximum coefficient loops' convergence controls were set to 1 and 10, respectively, while the timescale control was set to Coefficient Loops. 1E-04 was used as the convergence criterion. After one (1) iteration of the simulation, an initial values file was imported from a prior steady state simulation. The solver used this as a starting point for predicting flow field quantities (temperature, velocity, and pressure).

4. Results and Discussions

4.1 Mean Drying Temperature Result Analyses

The mean drying temperatures of all five inlet air temperatures were evaluated in order to ascertain the optimum range of cabinet dryer temperatures and drying times required to dry the fish properly without causing the fish to crack or damage, which may be as a result of too high inlet temperature or too long drying time. Reference data acquired online on fish drying (Small Scale Drying of Fish, ILO, 1982) comments that effective fish drying is achieved within the temperature range of 25 degrees Celsius (298K) to 45 degrees Celsius (328K). This ideal temperature range, given mathematically as $298K \leq T \leq 328K$, serves as a basis for comparing the mean drying temperature results obtained from the simulation with the drying time so as to obtain the best time for drying the fish. Drying temperatures above the ideal specified range would be deemed unfit to dry the fish and, as such, would result in the cracking of the fish, thereby causing damage to it. The table below shows the combined data of all five inlet air temperatures.

Table 4- Combine Result for the inlet temperature between 35ºC and 55ºC

35ºC (308K) INLET TEMP	40ºC (313K) INLET TEMP.	45ºC (318K) INLET TEMP.	50ºC (323K) INLET TEMP.	55ºC (328K) INLET TEMP.
TIME (MINS)	MEAN DRYING TEMP (K)	MEAN DRYING TEMP (K)	MEAN DRYING TEMP (K)	MEAN DRYING TEMP (K)
0	298.00	298.00	298.00	298.00
10	297.96	298.32	299.27	300.23
20	299.24	300.11	301.56	303.00
30	300.72	302.19	304.21	306.24
40	302.00	303.94	306.46	308.97
50	302.89	305.20	308.06	310.93
60	303.56	306.14	309.28	312.41
70	**304.07**	**306.85**	**310.19**	**313.52**
80	304.45	307.37	310.87	314.35
90	304.73	307.77	311.38	314.97
100	304.93	308.07	311.77	315.44
110	305.09	308.30	312.07	315.81
120	305.21	308.48	312.29	316.08

Figure 3- Plot of Mean Drying Temperatures against Time for All Inlet Air Temperatures

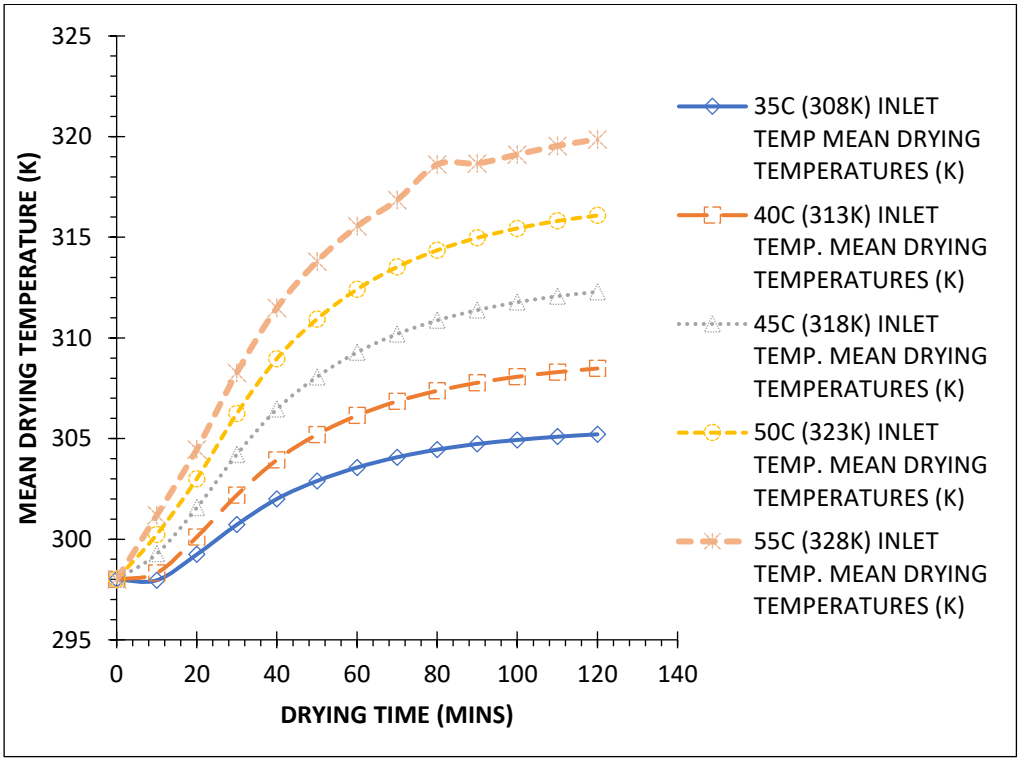

The datum temperature is taken to be 25 degrees Celsius. Drying will commence when the mean drying temperature rises above the datum temperature. Inlet air temperatures ranging from 35 degrees Celsius to 55 degrees Celsius were simulated for a time interval of 10 minutes to 120 minutes. As highlighted in Table 3 and Figure 3 above, the ideal drying time for the fish which satisfies the conditions for efficient fish drying for all five inlet air temperatures of the fish is 70 minutes. At these inlet air temperatures and drying times, the fish can be adequately dried without the negative effect of fish damage such as flaking or breakage. For drying times exceeding 70 minutes and an inlet air temperature of 55 degrees Celsius, it is observed that the mean cabinet drying temperature exceeds the range required for fish drying. At this point, there exists a high tendency for the fish to be damaged due to extreme loss of moisture and subsequent flaking. Furthermore, it is observed that the inlet air temperature of 55 degrees Celsius attains higher mean drying temperatures in less time as compared to the other four inlet air temperatures. At higher drying temperatures, the rate of convective heat transfer is high, and thus the drying process is faster. Furthermore, it can be observed that it takes about 120 minutes for the inlet air temperature of 50 degrees Celsius to attain a cabinet drying temperature of 316K (43°C), while it takes only 70 minutes for the inlet air temperature of 55 degrees Celsius to attain the same temperature. This is more significant due to the fact that with an increase of only 5 degrees Celsius in the inlet air temperature, there is a faster drying process, which thus helps to conserve heat energy supply costs for the cabinet dryer.

4.2 Visualization of result for each inlet temperature

Figure 4(a) through 4(j) visualize the temperature distribution contour plots of the air (fluid domain) within the drier at different inlet air temperatures and time intervals along the center of the dryer (YZ plane, X=0m). As displayed in the Figure 4 below, as the heated air (red color) is conveyed through the drier inlets which is slightly positioned below the fish domain (blue color), the temperature around the fish domain increases upwardly with the drying time.

Figure 4(a)-Temperature contour for 35°C, T=40mins, X=0m

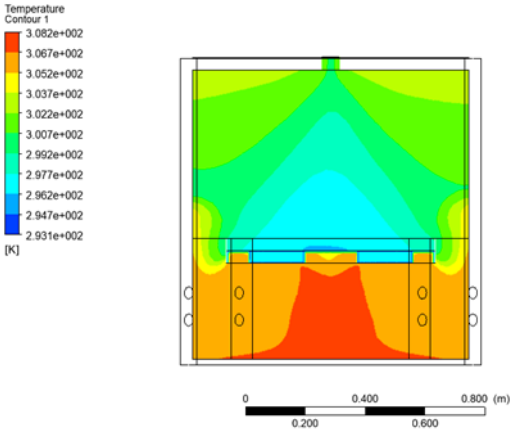

Figure 4(b)-Temperature contour for 35°C, T=70mins, X=0m

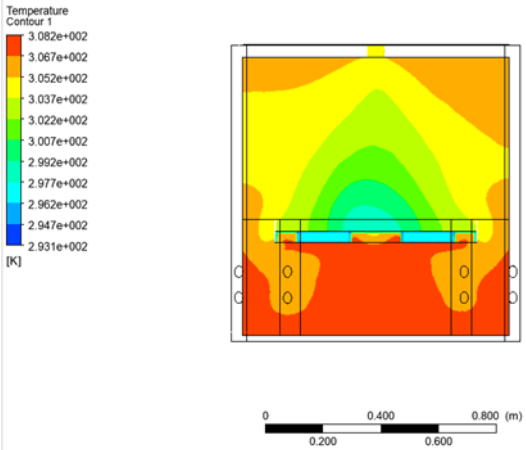

Figure 4(c)-Temperature contour for 40°C, T=40mins, X=0m

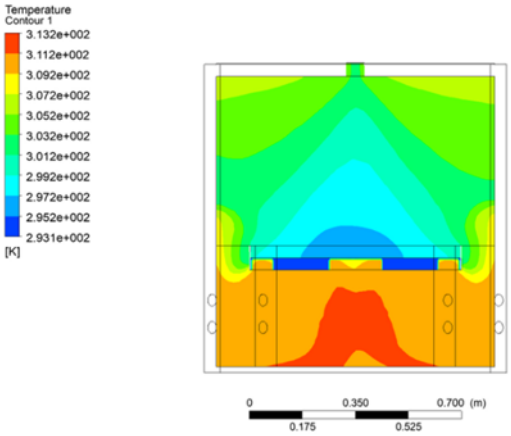

Figure 4(d)-Temperature contour for 40°C, T=70mins, X=0m

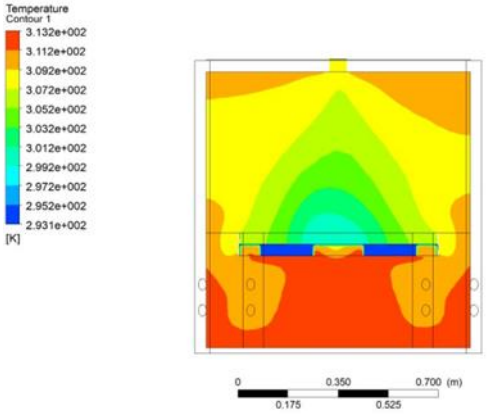

Figure 4(e)-Temperature contour for 45°C, T=40mins, X=0m

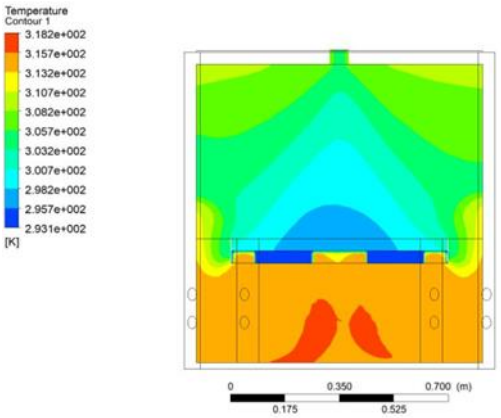

Figure 4(f)-Temperature contour for 45°C, T=70mins, X=0m

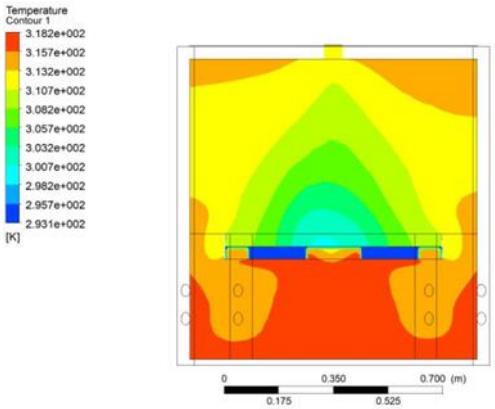

Figure 4(g)-Temperature contour for 50°C, T=40mins, X=0m

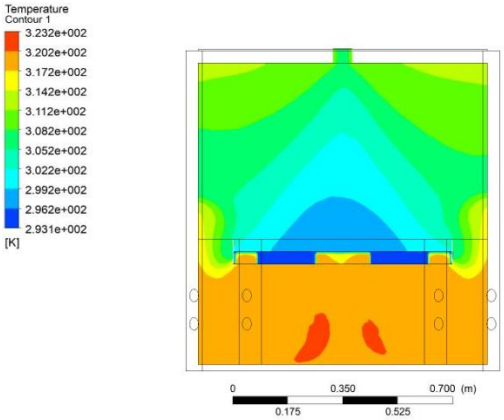

Figure 4(h)-Temperature contour for 50°C, T=70mins, X=0m

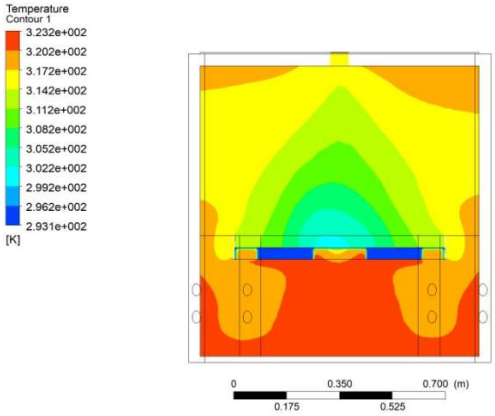

Figure 4(i)-Temperature contour for 55°C, T=40mins, X=0m	Figure 4(j)-Temperature contour for 55°C, T=70mins, X=0m
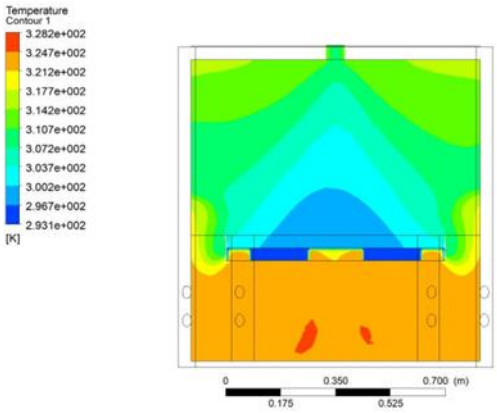	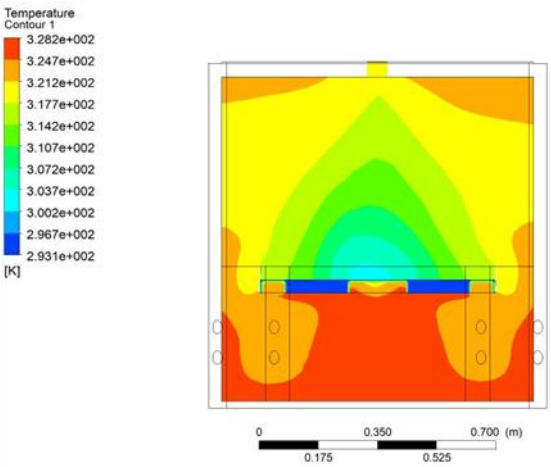

5. Conclusion

The utilization of the hot inlet air, which causes a forced convective heat transfer, is a very effective method for carrying out faster fish drying than the conventional method of drying. The mean cabinet drying temperature is a very good reference point for the drying process taking place within the dryer. Since proper fish drying can be effectively carried out within a specific temperature range and time, it is pertinent to study the effect that the cabinet air temperature has on the fish. Also, the presence of the rotary table within the dryer enables the efficient distribution of hot air around the fish and in the cabinet. Conserving heat within the cabinet rotary dryer is a key feature as loss of heat during the drying process will result in longer drying times, which would further increase the cost of heat energy supply. Further analytical research using computational fluid dynamics tools on the cabinet rotary dryer would allow more advancements in the technology of fish drying.

References

Abd El-Hay, M. M. (2022). Processing and preparation of fish. *Postharvest and Postmortem Processing of Raw Food Materials*, 315–342. https://doi.org/10.1016/b978-0-12-818572-8.00008-5

Brasil Maia, C., Guimarães Ferreira, A., Cabezas-Gómez, L., De Morais Hanriot, S., de Morais Hanriot, S., & de Oliveira Martins, T. (2012). Simulation of the airflow inside a hybrid dryer. *International Journal of Research and Reviews in Applied Sciences*, *10*(3), 382–389.

Çetinkaya, T., Ceylan, Z., Meral, R., Kılıçer, A., & Altay, F. (2021). A novel strategy for Au in food science: Nanoformulation in dielectric, sensory properties, and microbiological quality of fish meat. *Food Bioscience*, *41*, 101024. https://doi.org/10.1016/j.fbio.2021.101024

Dabadé, D. S., den Besten, H. M. W., Azokpota, P., Nout, M. J. R., Hounhouigan, D. J., & Zwietering, M. H. (2015). Spoilage evaluation, shelf-life prediction, and potential spoilage organisms of tropical brackish water shrimp (Penaeus notialis) at different storage temperatures. *Food Microbiology*, *48*, 8–16. https://doi.org/10.1016/j.fm.2014.11.005

Daramola, J. A., Fasakin, E. A., Adeparusi, E. O., & Daramola, J. (2016). Changes in physicochemical and sensory characteristics of smoke-dried fish species stored at ambient temperature. *African Journal of Food, Agriculture, Nutrition and Development*, *7*(6). https://doi.org/10.4314/ajfand.v7i6.

Darvishi, H., Azadbakht, M., Rezaeiasl, A., & Farhang, A. (2013). Drying characteristics of sardine fish dried with microwave heating. *Journal of the Saudi Society of Agricultural Sciences*, *12*(2), 121–127. https://doi.org/10.1016/j.jssas.2012.09.002

Dasin, D., Godi, N., & Kingsley, O. (2015). Experimental investigations of the performance of passive solar food dryer tested in Yola-Nigeria. *International Journal of Energy Engineering*, *5*(1), 9–15.

Horner, W. F. A. (1997). Preservation of fish by curing (drying, salting and smoking). *Fish Processing Technology*, 32–73. https://doi.org/10.1007/978-1-4613-1113-3_2

Legendre, R. (2011a). Artificial Drying of Cambodian Fish., *Journal of Fisheries Resources Board of Canada 18*(2), 147–162. https://doi.org/10.1139/f61-013

Legendre, R. (2011b). Artificial Drying of Salt Fish by Thermocouple Control. *Journal of Fisheries Resources Board of Canada*, *15*(4), 543–554. https://doi.org/10.1139/F58-027

Li, Z., Zhong, H., Tang, R., Liu, T., Gao, W., & Zhang, Y. (2006). Experimental investigation on solar drying of salted greengages. *Renewable Energy*, *31*(6), 837–847. https://doi.org/10.1016/j.renene.2005.05.008

Miketinac, M. J., Sokhansanj, S., & Tutek, Z. (1992). Determination of Heat and Mass Transfer Coefficients in Thin Layer Drying of Grain. *Transactions of the ASAE*, *35*(6), 1853–1858. https://doi.org/10.13031/2013.28806

Pelegrina, A. H., Elustondo, M. P., & Urbicain, M. J. (1998). Design of a semi-continuous rotary drier for vegetables. *Journal of Food Engineering*, *37*(3), 293–304. https://doi.org/10.1016/s0260-8774(98)00082-x

Pelegrina, A. H., Elustondo, M. P., & Urbicain, M. J. (1999). Rotary semi-continuous drier for vegetables: effect of air recycling. *Journal of Food Engineering*, *41*(3–4), 215–219. https://doi.org/10.1016/s0260-8774(99)00093-x

Rathod, N. B., Ranveer, R. C., Benjakul, S., Kim, S. K., Pagarkar, A. U., Patange, S., & Ozogul, F. (2021). Recent developments of natural antimicrobials and antioxidants on fish and fishery food products. *Comprehensive Reviews in Food Science and Food Safety*, *20*(4), 4182–4210. https://doi.org/10.1111/1541-4337.12787

Sarsilmaz, C., Yildiz, C., & Pehlivan, D. (2000). Drying of apricots in a rotary column cylindrical dryer (RCCD) supported with solar energy. *Renewable Energy*, *21*(2), 117–127. https://doi.org/10.1016/s0960-1481(00)00077-x

Shamshad, S. I., Kher-Un-Nisa, Riaz, M., Zuberi, R., & Qadri, R. B. (1990). Shelf Life of Shrimp (Penaeus merguiensis) Stored at Different Temperatures. *Journal of Food Science*, *55*(5), 1201–1205. https://doi.org/10.1111/j.1365-2621.1990.tb03898.x

Shenderyuk, V. I., & Bykowski, P. J. (2020). Salting and Marinating of Fish. In *Seafood: Resources, Nutritional Composition, and Preservation* (1st Edition, pp. 147–162). CRC Press. https://doi.org/10.1201/9781003068419-11

Singh, A., Mittal, A., & Benjakul, S. (2022). Undesirable discoloration in edible fish muscle: Impact of indigenous pigments, chemical reactions, processing, and its prevention. *Comprehensive Reviews in Food Science and Food Safety*, *21*(1), 580–603. https://doi.org/10.1111/1541-4337.12866

Smolka, J., Nowak, A. J., & Rybarz, D. (2010). Improved 3-D temperature uniformity in a laboratory drying oven based on experimentally validated CFD computations. *Journal of Food Engineering*, *97*(3), 373–383. https://doi.org/10.1016/j.jfoodeng.2009.10.032

Tavares, J., Martins, A., Fidalgo, L. G., Lima, V., Amaral, R. A., Pinto, C. A., … Saraiva, J. A. (2021). Fresh Fish Degradation and Advances in Preservation Using Physical Emerging Technologies. *Foods 2021, Vol. 10, Page 780*, *10*(4), 780. https://doi.org/10.3390/foods10040780

Tesfamariam, D. A., Bayray, M., Tesfay, M., & Hagos, F. Y. (2015). Modeling and experiment of solar crop dryer for rural application. *Journal of Chemical and Pharmaceutical Sciences*, (9), 2115.

Tzempelikos, D. A., Bardakas, A. V, Vouros, A. P., Tsepenekas, D. G., Christoloukas, D. A., Filios,

A. E., & Margaris, D. P. (2013). Design, construction and performance evaluation of a new laboratory convective dryer. *5th International Conference on Experiments/Process/System Modeling/Simulation and Optimization* . Athens. Retrieved from http://nemertes.library.upatras.gr/jspui/handle/10889/6257

Zhu, Y., Chen, X., Pan, N., Liu, S., Su, Y., Xiao, M., … Liu, Z. (2022). The effects of five different drying methods on the quality of semi-dried Takifugu obscurus fillets. *LWT*, *161*, 113340. https://doi.org/10.1016/j.lwt.2022.113340